ISSN: 2350-0328

International Journal of Advanced Research in Science, Engineering and Technology

Vol. 2, Issue 11 , November 2015

# Influence of MHD and wall properties on the peristaltic transport of a Williamson fluid through porous medium

**Dheia G. Salih Al-Khafajy , Ahmed M. Abdulhadi**

Department of Mathematics, College of Computer Science and Mathematics, University of Al-Qadisiyah, Iraq.
Department of Mathematics, College of Science, University of Baghdad, Baghdad-Iraq.

**ABSTRACT:** This work concerns the peristaltic flow of a Williamson fluid model through porous medium under combined effects of MHD and wall properties. The assumptions of Reynolds number and long wavelength is investigated. The flow is investigated in a wave frame of reference moving with velocity of the wave. The perturbation series in terms of the Weissenberg number ($We$ <1) was used to obtain explicit forms for velocity field and stream function . The effects of thermal conductivity, Grashof number, Darcy number, magnet, rigidity, stiffness of the wall and viscous damping force parameters on velocity, temperature and stream function have been studied.

**KEYWORDS**: MHD, Peristaltic transport, Williamson fluid, Porous medium.

## I. INTRODUCTION

Peristaltic flows have attracted the interest of a number of researchers because of wide applications in physiology and industry. Particularly, the occurrence of such flows are quite prevalent in biological organs; for instance, in urine transport from kidney to bladder, in movement of ovum in the fallopian tubes, in passage of food through oesophagus and many others. In industrial applications, these flows occur in blood pumps in heart-lung machine, in sanitary fluid transport and transport of corrosive fluids. Since, the pioneering works of Latham [1] and Shapiro et al. [2] a number of analytical, numerical and experimental (Fung and Yih, [3]; Jaffrin, [4]; Brown and Hung, [5]; Takabatake and Ayukawa, [6]; Takabatake et al., [7]; Ramachandra Rao and Usha, [8]; Subba Reddy et al., [9]) studies of peristaltic flows of different fluids have been reported under different conditions with reference to physiological and mechanical situations.

Several researchers considered the fluid to behave like a Newtonian fluid for physiological peristalsis including the flow of blood in arterioles. But such a model cannot be suitable for blood flow unless the non-Newtonian nature of the fluid is included in it. The non-Newtonian peristaltic flow using a constitutive equation for a second order fluid has been investigated by Siddiqui et al. [10] for a planar channel and by Siddiqui and Schwarz [11] for an axisymmetric tube. They have performed a perturbation analysis with a wave number, including curvature and inertia effects and have determined range of validity of their perturbation solutions. The effects of third order fluid on peristaltic transport in a planar channel were studied by Siddiqui et al. [12] and the corresponding axisymmetric tube results were obtained by Hayat et al. [13]. Haroun [14] studied peristaltic transport of third order fluid in an asymmetric channel. Subba Reddy et al. [15] studied the peristaltic flow of a power-law fluid in an asymmetric channel. Peristaltic motion of a Williamson fluid in an asymmetric channel was studied by Nadeem and Akram [16].

Further an interesting fact is that in oesophagus, the movement of food is due to peristalsis. The food moves from mouth to stomach even when upside down. Oesophagus is a long muscular tube commences at the neck opposite the long border of cricoids cartilage and extends from the lower end of the pharynx to the cardiac orifice of the stomach. The swallowing of the food bolus takes place due to the periodic contraction of the esophageal wall. Pressure due to reflexive contraction is exerted on the posterior part of the bolus and the anterior portion experiences relaxation so that the bolus moves ahead. The contraction is practically not symmetric, yet it contracts to zero lumen and squeezes it marvelously without letting any part of the food bolus slip back in the opposite direction. This shows the mportance of peristalsis in human beings. Mitra and Prasad [17] studied the influence of wall properties on the Poiseuille flow

ISSN: 2350-0328

International Journal of Advanced Research in Science, Engineering and Technology

Vol. 2, Issue 11 , November 2015

under peristalsis. Mathematical model for the esophageal swallowing of a food bolus is analyzed by Mishra and Pandey [18]. Kavitha et al. [19] analysed the peristaltic flow of a micropolar fluid in a vertical channel with longwave length approximation. Reddy et al. [20] studied the effect of thickness of the porous material on the peristaltic pumping when the tube wall is provided with non-erodible porous lining. Lakshminarayana et al. [21] studied the peristaltic pumping of a conducting fluid in a channel with a porous peripheral layer. Radhakrishnamacharya and Srinivasulu [22] studied the influence of wall properties on

peristaltic transport with heat transfer. Rathod et al. [23] studied the influence of wall properties on MHD peristaltic transport of dusty fluid. A new model for study the effect of wall properties on peristaltic transport of a viscous fluid has been investigated by Mokhtar and Haroun [24], Srinivas et al. [25] studied the effect of slip, wall properties and heat transfer on MHD peristaltic transport. Sreenadh et al. [26] studied the effects of wall properties and heat transfer on the peristaltic transport of food bolus through oesophagus. Al-Khafajy and Abdulhadi [27] analyzed the Effects of MHD and wall properties on the peristaltic transport of a Jeffrey fluid through porous medium channel.

Motivated by this, we consider a mathematical model to study the peristaltic flow of a Williamson fluid under the effect of magnetohydrodynamic and wall properties through porous medium. The results are analyzed for different values of parameters namely Grashof number, Darcy number, thermal conductivity, magnet, rigidity, stiffness and viscous damping forces of the channel wall through porous medium.

## II. MATHEMATICAL FORMULATION

Consider the peristaltic flow of an incompressible Williamson fluid in a flexible channel with flexible induced by sinusoidal wave trains propagating with constant speed c along the channel walls.

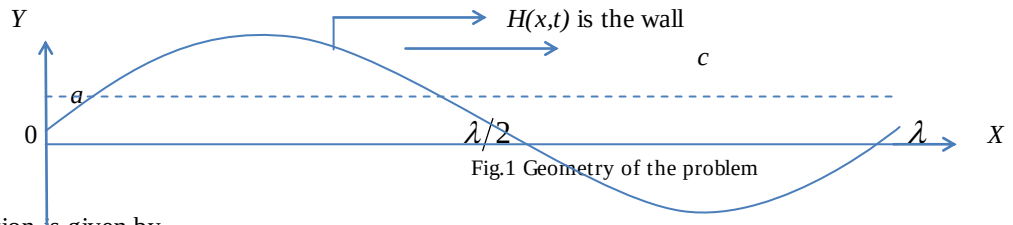


Fig.1 Geometry of the problem

The wall deformation is given by

$$H(\bar{x},\bar{t}) = a - \bar{\phi}\cos^2\frac{\pi}{\lambda}(\bar{x}-c\bar{t}) \qquad (1)$$

where $\bar{h}$, $\bar{x}$, $\bar{t}$, $\bar{\phi}$, $\lambda$ and $c$ represent transverse vibration of the wall, axial coordinate, time, half width of the channel, amplitude of the wave, wavelength and wave velocity respectively.

The basic equations governing the non-Newtonian incompressible Williamson fluid are given by:
The continuity equation is given by:

$$\frac{\partial\bar{u}}{\partial\bar{x}} + \frac{\partial\bar{v}}{\partial\bar{y}} = 0, \qquad (2)$$

The momentum equations are:

$$\rho\left(\frac{\partial\bar{u}}{\partial\bar{t}} + \bar{u}\frac{\partial\bar{u}}{\partial\bar{x}} + \bar{v}\frac{\partial\bar{u}}{\partial\bar{y}}\right) = -\frac{\partial\bar{p}}{\partial\bar{x}} + \frac{\partial\bar{\tau}_{\bar{x}\bar{x}}}{\partial\bar{x}} + \frac{\partial\bar{\tau}_{\bar{x}\bar{y}}}{\partial\bar{y}} + \rho g\alpha(T-T_0) - \sigma B_0^2\bar{u} - \frac{\mu_0}{k}\bar{u}, \qquad (3)$$

$$\rho\left(\frac{\partial\bar{v}}{\partial\bar{t}} + \bar{u}\frac{\partial\bar{v}}{\partial\bar{x}} + \bar{v}\frac{\partial\bar{v}}{\partial\bar{y}}\right) = -\frac{\partial\bar{p}}{\partial\bar{y}} + \frac{\partial\bar{\tau}_{\bar{y}\bar{x}}}{\partial\bar{x}} + \frac{\partial\bar{\tau}_{\bar{y}\bar{y}}}{\partial\bar{y}} - \frac{\mu_0}{k}\bar{v} \qquad (4)$$

The temperature equation is given by:

ISSN: 2350-0328
International Journal of Advanced Research in Science, Engineering and Technology
Vol. 2, Issue 11 , November 2015

$$\rho(\frac{\partial T}{\partial \bar{t}}+\bar{u}\frac{\partial T}{\partial \bar{x}}+\bar{v}\frac{\partial T}{\partial \bar{y}})=\frac{k}{c_p}(\frac{\partial^2 T}{\partial \bar{x}^2}+\frac{\partial^2 T}{\partial \bar{y}^2})+\Phi, \quad (5)$$

where $\bar{u}$ is the axial velocity, $\bar{v}$ transverse velocity, $\bar{y}$ transverse coordinate, $\rho$ fluid density, $\bar{p}$ pressure, $\mu_0$ fluid viscosity, $g$ acceleration due to gravity, $\alpha$ coefficient of linear thermal expansion of fluid, $B_0$ magnetic parameter, $T$ temperature, $c_p$ specific heat at constant pressure, $k$ is the thermal conductivity and $\Phi$ constant heat addition/absorption.

The constitutive equation for a Williamson fluid model [4], is:

$$\bar{\tau}=-[\mu_\infty+(\mu_0+\mu_\infty)(1-\Gamma\dot{\bar{\gamma}})^{-1}]\dot{\bar{\gamma}} \quad (6)$$

Where $\tau$ is the extra stress tensor, $\mu_\infty$ is the infinite shear rate viscosity, $\mu_0$ is the zero shear rate viscosity, $\Gamma$ is the time constant and $\dot{\gamma}$ is defined as

$$\dot{\gamma}=\sqrt{\frac{1}{2}\sum_i\sum_j\dot{\gamma}_{ij}\dot{\gamma}_{ji}}=\sqrt{\frac{1}{2}\Pi} \quad (7)$$

Here $\Pi$ is the second invariant stress tensor. We consider in the constitutive equation (6) the case for which $\mu_\infty$ = 0 and $\Gamma\dot{\gamma}$ < 1 so we can write

$$\bar{\tau}=-\mu_0(1+\Gamma\dot{\bar{\gamma}})]\dot{\bar{\gamma}} \quad (8)$$

The above model reduces to Newtonian for $\Gamma$ = 0.

The velocity and temperatures at the central line and the wall of the peristaltic channel are given as:

$T=T_0$ at $\bar{y}=0$

$T=T_1$ at $\bar{y}=\bar{h}$

where $T_0$ is the temperature at centre is line and $T_1$ is the temperature on the wall of peristaltic channel.

The governing equation of motion of the flexible wall may be expressed as:

$$L^*=\bar{p}-\bar{p}_0 \quad (9)$$

where $L^*$ is an operator, which is used to represent the motion of stretched membrane with viscosity damping forces such that

$$L^*=-\kappa\frac{\partial^2}{\partial x^2}+m_1\frac{\partial^2}{\partial t^2}+C\frac{\partial}{\partial t} \quad (10)$$

where $\kappa$ is the elastic tension in the membrane, $m_1$ is the mass per unit area, $C$ is the coefficient of viscous damping forces.

Continuity of stress at $y=\bar{h}$ and using momentum equation, yield

$$\frac{\partial}{\partial \bar{x}}L^*(\bar{h})=\frac{\partial \bar{p}}{\partial \bar{x}}=\frac{\partial \bar{\tau}_{\bar{x}\bar{x}}}{\partial \bar{x}}+\frac{\partial \bar{\tau}_{\bar{x}\bar{y}}}{\partial \bar{y}}-\rho(\frac{\partial \bar{u}}{\partial \bar{t}}+\bar{u}\frac{\partial \bar{u}}{\partial \bar{x}}+\bar{v}\frac{\partial \bar{u}}{\partial \bar{y}})+\rho g\alpha(T-T_0)-\sigma B_0^2\bar{u}-\frac{\mu_0}{k}\bar{u} \quad (11)$$

In order to simplify the governing equations of the motion, we may introduce the following dimensionless transformations as follows:

ISSN: 2350-0328

International Journal of Advanced Research in Science, Engineering and Technology

Vol. 2, Issue 11 , November 2015

$$\left.\begin{aligned} x=\frac{\bar{x}}{\lambda}, y=\frac{\bar{y}}{a}, \delta=\frac{a}{\lambda}, u=\frac{\bar{u}}{c}, v=\frac{\bar{v}}{c\delta}, t=\frac{c\bar{t}}{\lambda}, \phi=\frac{\bar{\phi}}{a}, We=\frac{\Gamma c}{a}, Da=\frac{k}{a^2}, \\ p=\frac{a^2\bar{p}}{\mu_0\lambda c}, Gr=\frac{gpa^2\alpha(T_1-T_0)}{c\mu_0{}^2}, \theta=\frac{T-T_0}{T_1-T_0}, M^2=\frac{\sigma B_0^2 a^2}{\mu_0}, \beta=\frac{a^2\Phi}{k(T_1-T_0)}, \\ \mathrm{Re}=\frac{\rho c a}{\mu_0}, \mathrm{Pr}=\frac{\mu_0 c_p}{k}, \tau_{xx}=\frac{\lambda}{\mu_0 c}\bar{\tau}_{\bar{x}\bar{x}}, \tau_{xy}=\frac{a}{\mu_0 c}\bar{\tau}_{\bar{x}\bar{y}}, \tau_{yy}=\frac{\lambda}{\mu_0 c}\bar{\tau}_{\bar{y}\bar{y}}, \dot{\gamma}=\frac{a\bar{\dot{\gamma}}}{c} \end{aligned}\right\} \quad (12)$$

where $\delta$ is the length of the channel, *We* Weissenberg number, *Da* Darcy number, Re Reynolds number, *Gr* Grashof number, $\theta$ dimensionless temperature, $M$ magnetic parameter, $\beta$ dimensionless heat source/sink parameter and Pr Prandtl number.

Substituting (12) into equations (1)-(11), we obtain the following non-dimensional equations and boundary conditions:

$$h(x,t)=1-\phi\cos^2\pi(x-t) \quad (13)$$

$$\frac{\partial u}{\partial x}+\frac{\partial v}{\partial y}=0 \quad (14)$$

$$\mathrm{Re}\,\delta\left(\frac{\partial u}{\partial t}+u\frac{\partial u}{\partial x}+v\frac{\partial u}{\partial y}\right)=-\frac{\partial p}{\partial x}+\delta^2\frac{\partial \tau_{xx}}{\partial x}+\frac{\partial \tau_{xy}}{\partial y}+\frac{\rho g a^2\alpha(T-T_0)}{\mu_0 c}\theta-M^2u-\frac{1}{Da}u \quad (15)$$

$$\mathrm{Re}\,\delta^3\left(\frac{\partial v}{\partial t}+u\frac{\partial v}{\partial x}+v\frac{\partial v}{\partial y}\right)=-\frac{\partial p}{\partial x}+\delta^2\left(\frac{\partial \tau_{yx}}{\partial x}+\frac{\partial \tau_{yy}}{\partial y}\right)-\frac{\delta^2}{Da}v \quad (16)$$

$$\frac{\mathrm{Re}\,\delta\,\mathrm{Pr}}{(T_1-T_0)}\left(\frac{\partial}{\partial t}+u\frac{\partial}{\partial x}+v\frac{\partial}{\partial y}\right)(\theta(T_1-T_0)+T_0)=\delta^2\frac{\partial^2\theta}{\partial x^2}+\frac{\partial^2\theta}{\partial y^2}+\beta \quad (17)$$

$$\delta^2\frac{\partial \tau_{xx}}{\partial x}+\frac{\partial \tau_{xy}}{\partial y}+Gr\theta-\left(M^2+\frac{1}{Da}\right)u-\mathrm{Re}\,\delta\left(\frac{\partial u}{\partial t}+u\frac{\partial u}{\partial x}+v\frac{\partial u}{\partial y}\right)=E_1\frac{\partial^3 h}{\partial x^3}+E_2\frac{\partial^3 h}{\partial x\partial t^2}+E_3\frac{\partial^2 h}{\partial x\partial t} \quad (18)$$

where

$$\left.\begin{aligned} \tau_{xx}=-2[1+We\dot{\gamma}]\frac{\partial u}{\partial x} \quad , \quad \tau_{xy}=-[1+We\dot{\gamma}]\left(\frac{\partial u}{\partial y}+\delta^2\frac{\partial v}{\partial x}\right) \\ \tau_{yy}=-2[1+We\dot{\gamma}]\frac{\partial v}{\partial y} \quad , \quad \dot{\gamma}=\sqrt{2\delta^2\left(\frac{\partial u}{\partial x}\right)^2+\left(\frac{\partial u}{\partial y}+\delta^2\frac{\partial v}{\partial x}\right)^2+2\delta^2\left(\frac{\partial v}{\partial y}\right)^2} \end{aligned}\right\} \quad (19)$$

The corresponding boundary conditions are

$$\left.\begin{aligned} \frac{\partial u}{\partial y}=v=\theta=0 \qquad \text{at} \quad y=0 \\ u=0,\theta=1 \qquad \text{at} \quad y=h \end{aligned}\right\} \quad (20)$$

## III. SOLUTION OF THE PROBLEM

The general solution of the governing equations (14)-(18) in the general case seems to be impossible; therefore, we shall confine the analysis under the assumption of small dimensionless wave number. It follows that $\delta << 1$. In other words, we considered the long-wavelength approximation. Along to this assumption, equations (13)-(18) become:

$$h(x,t)=1-\phi\cos^2\pi(x-t) \quad (21)$$

ISSN: 2350-0328
International Journal of Advanced Research in Science, Engineering and Technology
Vol. 2, Issue 11 , November 2015

$$\frac{\partial u}{\partial x}+\frac{\partial v}{\partial y}=0 \tag{22}$$

$$\frac{\partial p}{\partial x}=\frac{\partial}{\partial y}\left(-[1+We\frac{\partial u}{\partial y}]\frac{\partial u}{\partial y}\right)+Gr\theta-(M^2+\frac{1}{Da})u \tag{23}$$

$$\frac{\partial p}{\partial y}=0 \tag{24}$$

$$\frac{\partial^2\theta}{\partial y^2}+\beta=0 \tag{25}$$

$$\frac{\partial}{\partial y}\left(-[1+We\frac{\partial u}{\partial y}]\frac{\partial u}{\partial y}\right)+Gr\theta-(M^2+\frac{1}{Da})u=E_1\frac{\partial^3 h}{\partial x^3}+E_2\frac{\partial^3 h}{\partial x\partial t^2}+E_3\frac{\partial^2 h}{\partial x\partial t} \tag{26}$$

The corresponding Stream function ($u=\partial\psi/\partial y, v=-\partial\psi/\partial x$) with boundary condition $\psi=0$ at $y=0$.
The exact solution of equation (25) with boundary condition given in equation (20) is

$$\theta=\frac{y}{h}+\frac{\beta}{2}(hy-y^2) \tag{27}$$

Equation (24) shows that $p$ dependents on *x* only. Equation (26) is non-linear and it is difficult to get a closed form solution. However for vanishing *We*, the boundary value problem is agreeable to an easy analytical solution. In this case the equation becomes linear and can be solved. Nevertheless, small $\Gamma$ suggests the use of perturbation technique to solve the non-linear problem. Accordingly, we write

$$\left.\begin{aligned}u&=u_0+Weu_1+We^2u_2+O(We^3)\\ \psi&=\psi_0+We\psi_1+We^2\psi_2+O(We^3)\end{aligned}\right\} \tag{28}$$

Substituting equations (28) into equation (26) with boundary conditions, then equating the like powers of *We*, we obtain

***A*- Zeroth-order system ($We^0$)**

$$\frac{\partial^2 u_0}{\partial y^2}+(M^2+\frac{1}{Da})u_0-Gr\theta=-\left(E_1\frac{\partial^3 h}{\partial x^3}+E_2\frac{\partial^3 h}{\partial x\partial t^2}+E_3\frac{\partial^2 h}{\partial x\partial t}\right) \quad \text{and} \quad \psi_0=\int u_0 dy \tag{29}$$

The associated boundary conditions are

$$\left.\frac{\partial u_0}{\partial y}\right|_{y=0}=u_0(h)=0 \text{ and } \psi_0=0 \text{ at } y=0 \tag{30}$$

***B*- First-order system ($We^1$)**

$$\frac{\partial^2 u_1}{\partial y^2}+(M^2+\frac{1}{Da})u_1=-2\frac{\partial u_0}{\partial y}\frac{\partial^2 u_0}{\partial y^2} \quad \text{and} \quad \psi_1=\int u_1 dy \tag{31}$$

The associated boundary conditions are

$$\left.\frac{\partial u_1}{\partial y}\right|_{y=0}=u_1(h)=0 \text{ and } \psi_1=0 \text{ at } y=0 \tag{32}$$

***C*- Second-order system ($We^2$)**

$$\frac{\partial^2 u_2}{\partial y^2}+(M^2+\frac{1}{Da})u_2=-2\left(\frac{\partial^2 u_1}{\partial y^2}\frac{\partial u_0}{\partial y}+\frac{\partial^2 u_0}{\partial y^2}\frac{\partial u_1}{\partial y}\right) \quad \text{and} \quad \psi_2=\int u_2 dy \tag{33}$$

The associated boundary conditions are

ISSN: 2350-0328

International Journal of Advanced Research in Science, Engineering and Technology

Vol. 2, Issue 11 , November 2015

$$\left.\frac{\partial u_2}{\partial y}\right|_{y=0} = u_2(h) = 0 \text{ and } \psi_2 = 0 \text{ at } y = 0 \tag{34}$$

Finally, the perturbation solutions up to second term for $u$ and $\psi$ are given by

$$u = u_0 + We u_1 + We^2 u_2 \tag{35}$$

$$\psi = \psi_0 + We\,\psi_1 + We^2 \psi_2 \tag{36}$$

## IV. RESULTS AND DISCUSSION

In this section, the numerical and computational results are discussed for the problem of an incompressible non-Newtonian the peristaltic flow of a Williamson fluid model through porous medium under combined effects of MHD and wall properties through the graphical illustrations. The numerical evaluations of the analytical results and some important results are displayed graphically in Figure 2-16. MATHEMATICA program is used to find out numerical results and illustrations. The analytical solutions of the momentum equation and temperature equation are obtained by using perturbation technique. All the obtained solutions are discussed graphically under the variations of various pertinent parameters in the present section. The trapping bolus phenomenon is also incorporated through sketching graphs of streamlines for various physical parameters.

Based on equation (35), Figures 2-6, illustrates the effects of the parameters $E_1$, $E_2$, $E_3$, *We*, *Gr*, $\beta$, *M*, *Da* and $\phi$ on the velocity. Figure 2, illustrates the effects of the parameters $E_1$ and $E_2$ on the velocity distribution function u vs. y. It is found that the velocity profile *u* rising up with the increasing effects of both the parameters $E_1$ and $E_2$, when $|y| < 0.8643$, and attains its maximum height at $y = 0$, the fluid velocity starts increasing and tends to be constant at the peristaltic walls, as specified by the boundary conditions. From figure 3, one can depict here that velocity decreases with increasing of $E_3$, while that velocity profile is rising up with increasing of the parameters *We*, when $|y| < 0.8643$. Figure 4, contains the behavior of *u* under the variation of *Gr* and $\beta$, one can depict here that *u* go down with the increasing effects of both the parameters *Gr* and $\beta$, when $|y| < 0.8643$. Figure 5, illustrates the effects of the parameters *M* and *Da* on velocity profile. One can depict here that velocity decreases with increasing of *Da*, while that velocity profile is rising up with increasing of *M*, when $|y| < 0.8643$. Figure 6, show that velocity distribution decreases with the increasing of $\phi$. Also at $\phi = 0.15$, $u > 0$ when $|y| < 0.8643$ and $u(0.8643) = 0$. At $\phi = 0.175$, $u > 0$ when $|y| < 0.8417$ and $u(0.8417) = 0$. At $\phi = 0.2$, $u > 0$ when $|y| < 0.8191$ and $u(0.8191) = 0$. And at $\phi = 0.225$, $u > 0$ when $|y| < 0.7965$ and $u(0.7965) = 0$, as specified by the boundary conditions.

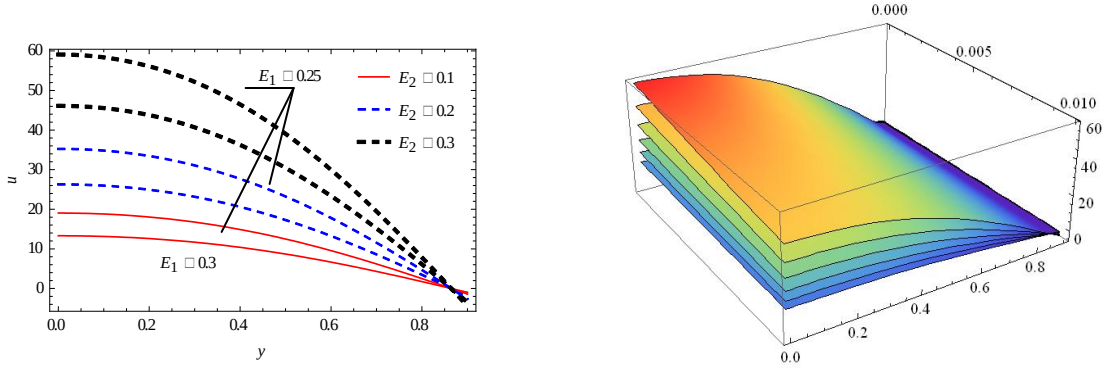


Fig. 2: Velocity profile for different values of $E_1$ and $E_2$ with $x = 0, t = 0.1, We = 0.05, E_3 = 0.1, Gr = 1, \phi = 0.15, \beta = 1, Da = 0.7, M = 0.9$.

ISSN: 2350-0328

International Journal of Advanced Research in Science, Engineering and Technology

Vol. 2, Issue 11 , November 2015

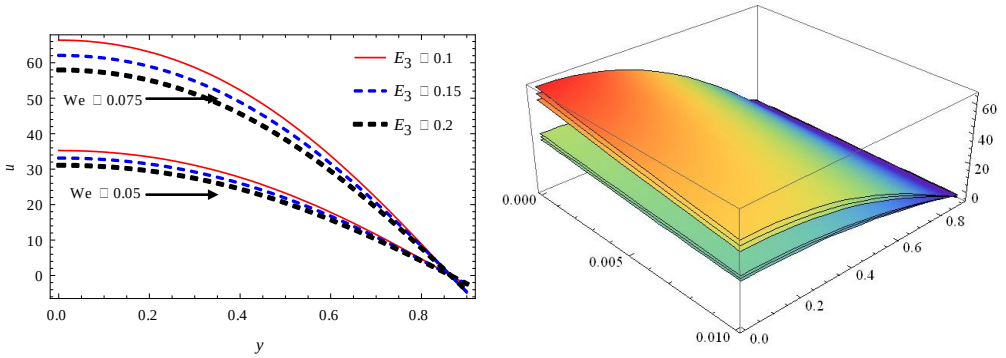


Fig. 3: Velocity profile for different values of *We* and $E_3$ with $x=0, t=0.1, E_1=0.3, E_2=0.2, \phi=0.15, Gr=1, \beta=1, Da=0.7, M=0.9$

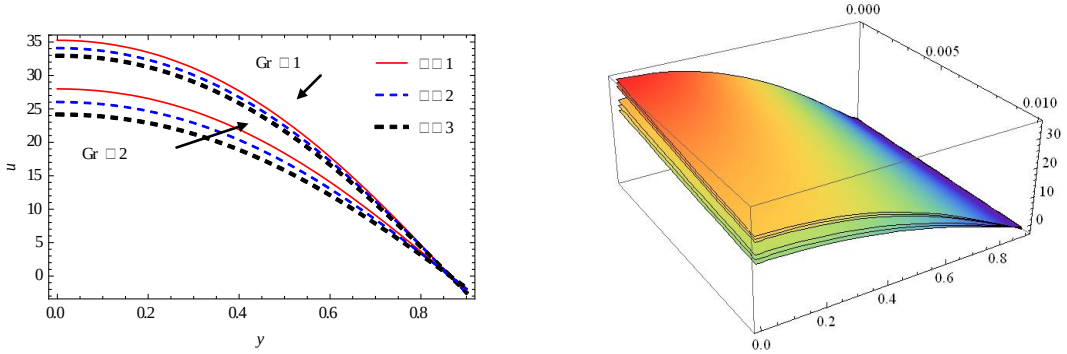


Fig. 4: Velocity profile for different values of $Gr$ and $\beta$ with $x=0, t=0.1, We=0.05, E_1=0.3, E_2=0.2, E_3=0.1, \phi=0.15, Da=0.7, M=0.9$

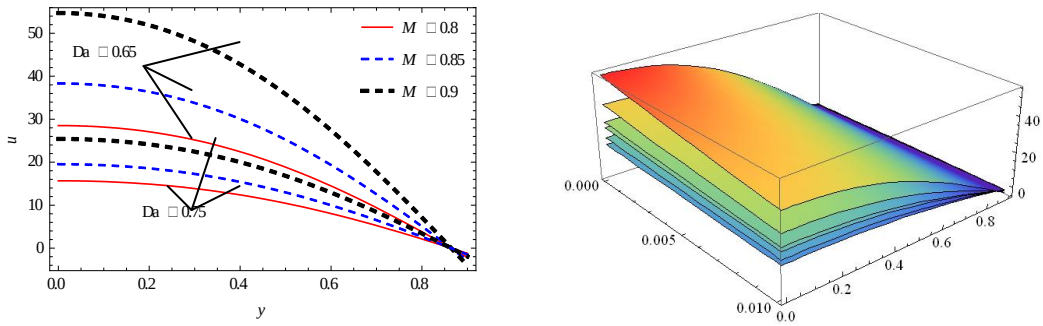


Fig. 5: Velocity profile for different values of *Da* and *M* with $x=0, t=0.1, We=0.05, E_1=0.3, E_2=0.2, E_3=0.1, \phi=0.15, Gr=1, \beta=1$

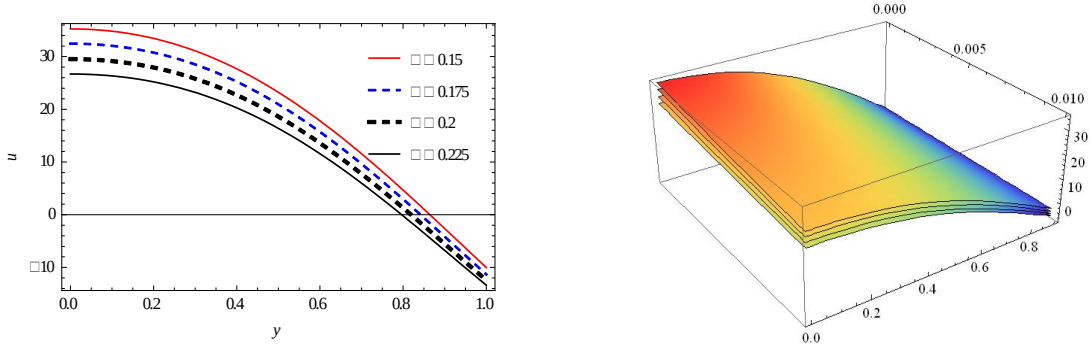

ISSN: 2350-0328
International Journal of Advanced Research in Science, Engineering and Technology
Vol. 2, Issue 11 , November 2015

Fig. 6: Velocity profile for different values of $\phi$ with $x=0, t=0.1, We=0.05, E_1=0.3, E_2=0.2, E_3=0.1, Gr=1, \beta=1, Da=0.7, M=0.9$

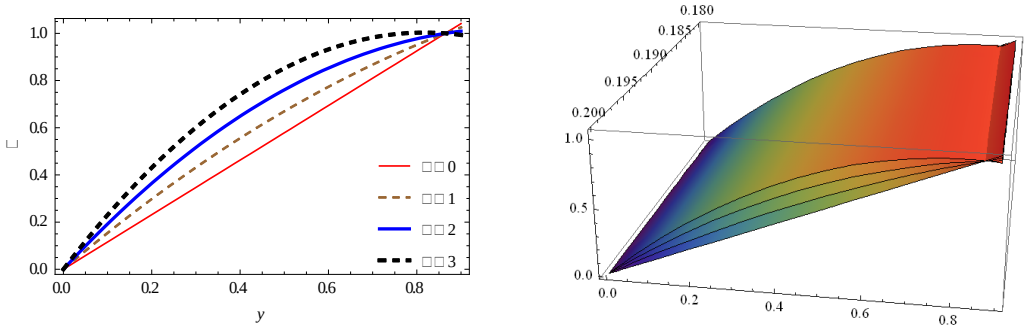


Fig. 7: Temperature distribution for different values of $\beta$ with $x=0, t=0.1, \phi=0.15$.

Based on equation (27), figure 7, shows that effects of the parameter $\beta$ on the temperature distribution function $\theta$. The temperature increases with the increase in $\beta$, when $|y| < 0.8643$, and $\theta(0.8643) = 1$ ( at $y = h = 0.8643$) as specified by the boundary conditions.

## V. TRAPPING PHENOMENON

The formation of an internally circulating bolus of fluid by closed streamlines is called trapping and this trapped bolus is pushed ahead along with the peristaltic wave.

Based on equation (36), the effects of $E_1$, $E_2$, $E_3$, *Gr*, $\beta$, *Da*, *M*, *We* and $\phi$ on trapping can be seen through figures 8-16, it is observed that the bolus move near the side walls. Figure 8, show that the size of the trapped bolus increase with the increase in $E_1$. Figure 9, is plotted, the effect of $E_2$ on trapping, the size of the trapped bolus increase with the increase in $E_2$. Figure 10, show that the size of the left trapped bolus increases with increase in $E_3$ where as the size of the right trapped bolus decreases with increase in $E_3$. The effect of Grashof number *Gr* on trapping is analyzed in figure 11. It can be concluded that the size of the trapped bolus in the left side of the channel decreases when *Gr* increases where as it has opposite behavior in the right hand side of the channel. Figure 12, show that the size of the left trapped bolus decreases with increase in $\beta$ where as the size of the right trapped bolus increases with increase in $\beta$. The influence of Darcy number *Da* on trapping is analyzed in figure 13. It shows that the size of the trapped bolus decreases with increase in *Da*. Figure 14, show that influence of *M* on trapping. It shows that the size of the trapped bolus increases with increase in *M*. The influence of Weissenberg number *We* on trapping is analyzed in figure 15. It shows that the size of the trapped bolus increases with increase in *We*. And the effect of $\phi$ on trapping is analyzed in figure 16. We notice that the size of the trapped bolus increases with increase $\phi$.

ISSN: 2350-0328

International Journal of Advanced Research in Science, Engineering and Technology

Vol. 2, Issue 11 , November 2015

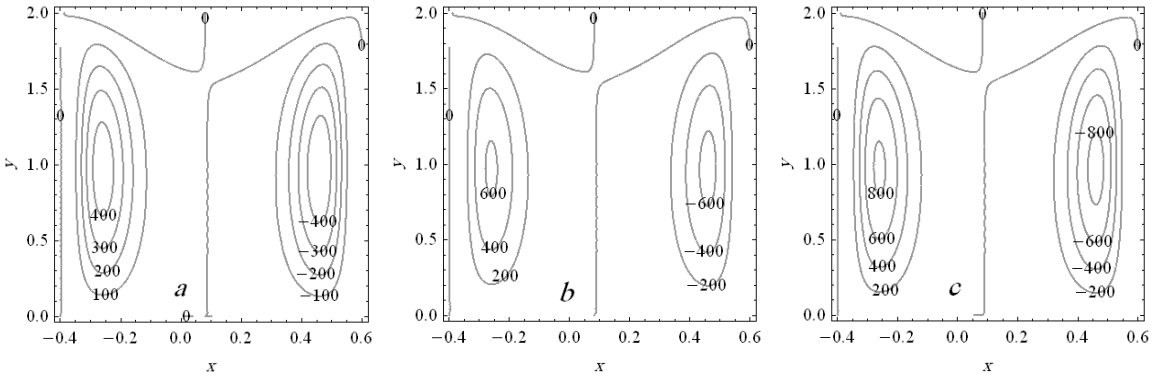


Fig. 8: Graph of the streamlines for three different values of $E_1$; (a) $E_1$= 0.25, (b) $E_1$= 0.3 and (c) $E_1$= 0.35 at $t = 0.1, We = 0.05, E_2 = 0.2, E_3 = 0.1, Da = 0.8, M = 0.9, Gr = 1, \phi = 0.15, \beta = 1$.

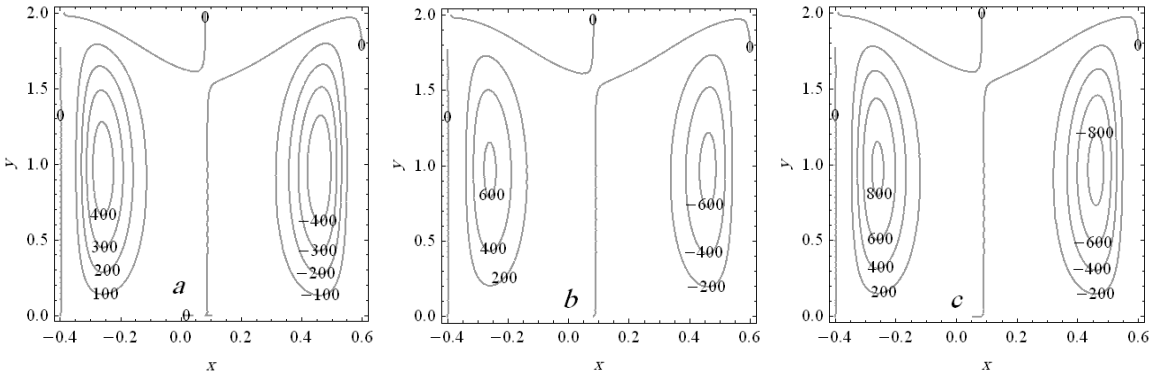


Fig. 9: Graph of the streamlines for three different values of $E_2$; (a) $E_2$= 0.15, (b) $E_2$= 0.2 and (c) $E_2$= 0.25 at $t = 0.1, We = 0.05, E_1 = 0.3, E_3 = 0.1, Da = 0.8, M = 0.9, Gr = 1, \phi = 0.15, \beta = 1$.

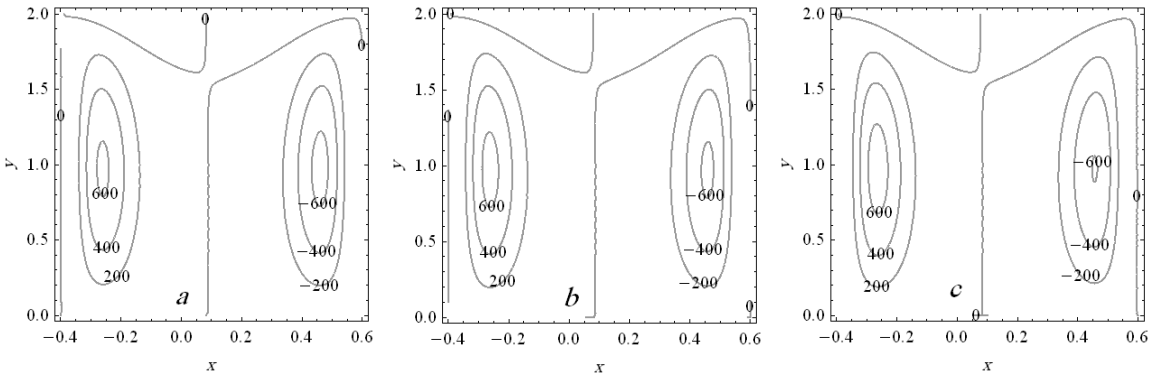


Fig. 10: Graph of the streamlines for three different values of $E_3$; (a) $E_3$= 0.1, (b) $E_3$= 0.15 and (c) $E_3$= 0.2 at $t = 0.1, We = 0.05, E_1 = 0.3, E_2 = 0.2, Da = 0.8, M = 0.9, Gr = 1, \phi = 0.15, \beta = 1$

ISSN: 2350-0328

International Journal of Advanced Research in Science, Engineering and Technology

Vol. 2, Issue 11 , November 2015

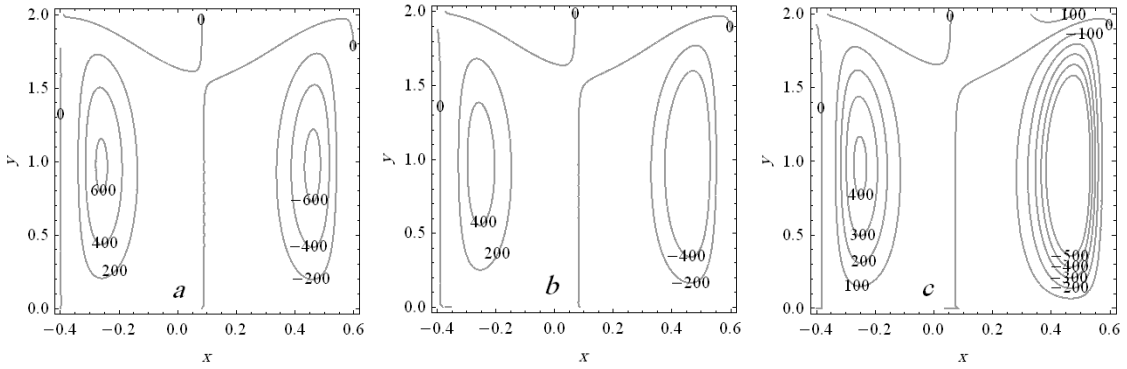


Fig. 11: Graph of the streamlines for three different values of $Gr$ ; (a) $Gr$ = 1, (b) $Gr$ = 2 and (c) $Gr$ = 3 at $t = 0.1, We = 0.05, E_1 = 0.3, E_2 = 0.2, E_3 = 0.1, Da = 0.8, M = 0.9, \phi = 0.15, \beta = 1$.

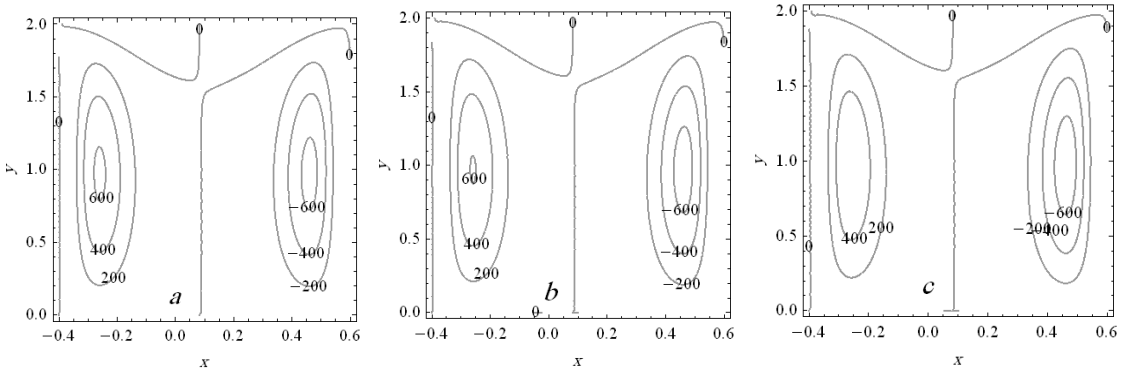


Fig. 12: Graph of the streamlines for three different values of $\beta$ ; (a) $\beta$ = 1, (b) $\beta$ = 2 and (c) $\beta$ = 3 at $t = 0.1, We = 0.05, E_1 = 0.3, E_2 = 0.2, E_3 = 0.1, Da = 0.8, M = 0.9, Gr = 1, \phi = 0.15$ .

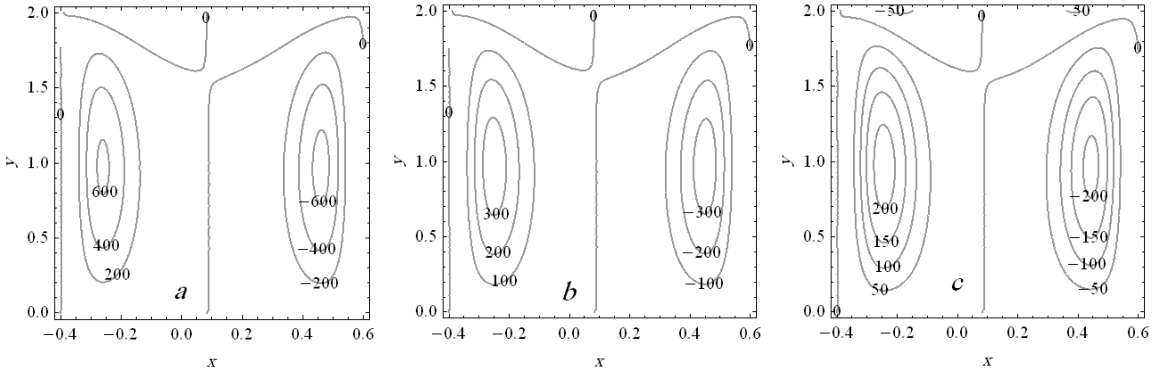


Fig. 13: Graph of the streamlines for three different values of $Da$; (a) $Da$ = 0.8, (b) $Da$ = 0.85 and (c) $Da$ = 0.9 at $t = 0.1, We = 0.05, E_1 = 0.3, E_2 = 0.2, E_3 = 0.1, M = 0.9, Gr = 1, \phi = 0.15, \beta = 1$.

ISSN: 2350-0328

International Journal of Advanced Research in Science, Engineering and Technology

Vol. 2, Issue 11 , November 2015

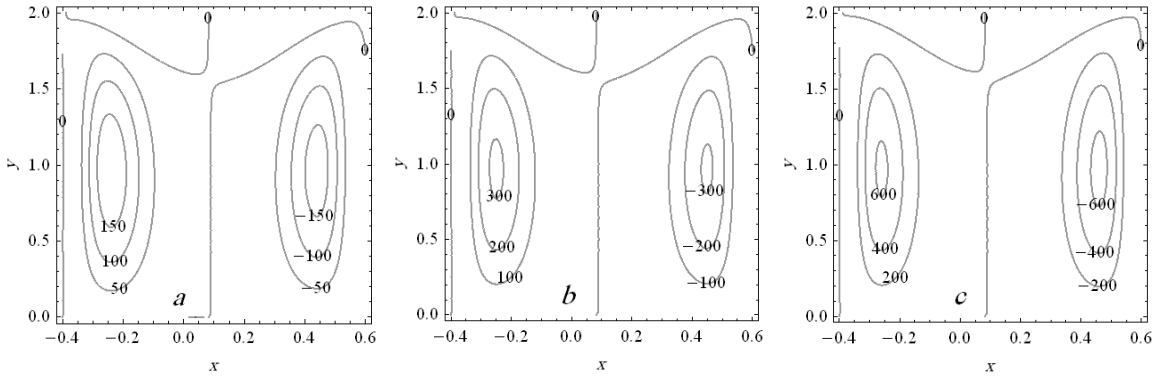


Fig. 14: Graph of the streamlines for three different values of $M$; (a) $M$ = 0.8, (b) $M$ = 0.85 and (c) $M$ = 0.9 at $t=0.1, We=0.05, E_1=0.3, E_2=0.2, E_3=0.1, Da=0.8, Gr=1, \phi=0.15, \beta=1$.

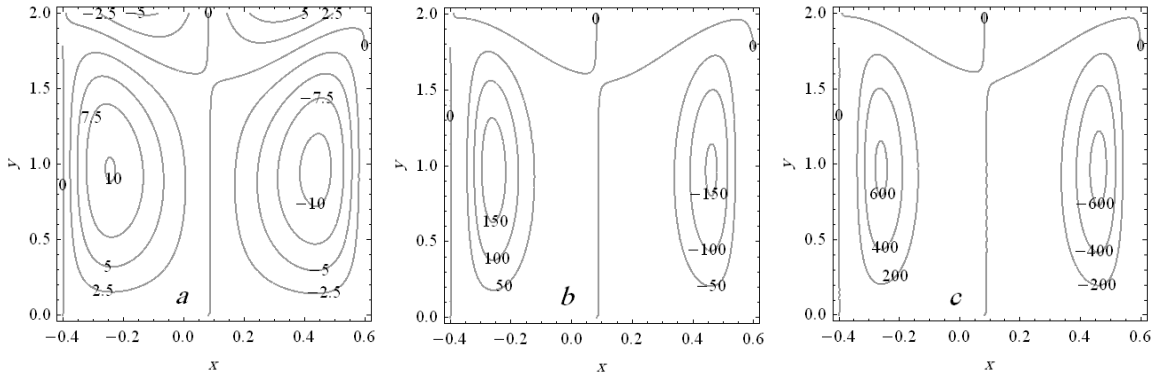


Fig. 15: Graph of the streamlines for three different values of $We$; (a) $We$ = 0, (b) $We$ = 0.025 and (c) $We$ = 0.05 at $t=0.1, E_1=0.3, E_2=0.2, E_3=0.1, Gr=1, Da=0.8, M=0.9, \phi=0.15, \beta=1$.

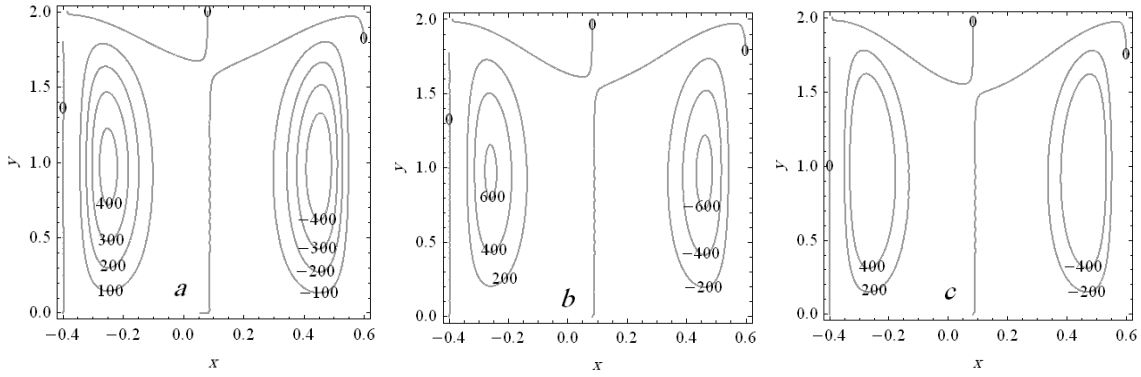


Fig. 16: Graph of the streamlines for three different values of $\phi$; (a) $\phi$ = 0.125, (b) $\phi$ = 0.15 and (c) $\phi$ = 0.175 at $t=0.1, We=0.05, E_1=0.3, E_2=0.2, E_3=0.1, Da=0.8, M=0.9, Gr=1, \beta=1$.

## VI. CONCLUDING REMARKS

The present study deals with the combined effect of MHD and wall properties on the peristaltic transport of a Williamson fluid in a two dimensional channel through porous medium. We obtained the analytical solution of the problem under long wavelength and low Reynolds number assumptions. The perturbation series in the Weissenberg number ($We$ < 1) was used to obtain explicit forms for velocity field and stream function per one wavelength. The results are analyzed for different values of pertinent parameters namely Grashof number, Darcy

ISSN: 2350-0328

International Journal of Advanced Research in Science, Engineering and Technology

Vol. 2, Issue 11 , November 2015

number, thermal conductivity, rigidity, stiffness, magnet and viscous damping forces of the channel wall through porous medium. From wall properties and type of fluid (Williamson), we observed that the bolus move near the side walls. The main findings can be summarized as follows:

1. The axial velocity increases with the increase in $E_1$, $E_2$, *We* and *M*, when $|y| < 0.8643$. Further, the axial velocity decreases with increase in $E_3$, *Gr*, $\beta$, *Da* and $\phi$.

2- The size of the trapped bolus increase with the increase in $E_1$, $E_2$, *M*, $\phi$ and *We*. While the size of the trapped bolus decreases with increase in *Da*.

3- The size of the left trapped bolus increases with increase in $E_3$ where as the size of the right bolus decreases with increase in $E_3$. And the size of the trapped bolus in the left side of the channel decreases when *Gr*, $\beta$ increases where as it has opposite behavior in the right hand side of the channel.

4. The coefficient of temperature increases with increasing values of thermal conductivity $\beta$.

## REFERENCES

[1] Latham T.W., Fluid motions in peristaltic pump, M. Sc. Thesis, Cambridge, Mass: MIT –Press, 1966.
[2] Shapiro A.H., Jaffrin M.Y., Weinberg S.L., Peristaltic pumping with long wavelengths at low Reynolds number, J. Fluid Mech., .37, pp. 799-825, 1969.
[3] Fung Y.C., Yih C.S., Peristaltic transport, Trans. ASME J. Appl. Mech., 35, pp. 669-675, 1968.
[4] Jaffrin M.Y., Inertia and streamline curvature effects on peristaltic pumping, Int. J. Eng. Sci., 11, pp. 681-699, 1973.
[5] Brown T.D., Hung T.K., Computational and experimental investigations of two- dimensional nonlinear peristaltic flows, J. Fluid Mech., 83, pp. 249-272, 1977.
[6] Takabatake S., Ayukawa K., Numerical study of two-dimensional peristaltic flow, J. Fluid Mech., 122, pp. 439-465, 1982.
[7] Takabatake S., Ayukawa K., Mori A., Peristaltic pumping in circular tubes: A numerical study of fluid transport and its efficiency, J. Fluid Mech., 193, pp. 267-283, 1988.
[8] Ramachan Rao A., Usha S., Peristaltic transport of two immiscible viscous fluid in a circular tube, J. Fluid Mech., 298, pp. 271-285, 1995.
[9] Subba Reddy M.V., Mishra M., Sreenadh S., Ramachandra Rao A., Influence of lateral walls on peristaltic pumping in a rectangular duct, Trans. ASME. Journal of Fluids Engineering, 127, pp. 824-827, 2005.
[10] Siddiqui A.M., Provost A., Peristaltic pumping of a second- order fluid in a planar channel, Rheol. Acta, 30, pp. 249-262, 1991.
[11] Siddiqui A.M., Schwarz W.H., Peristaltic flow of a second order fluid in tubes, J. Non-Newtonian Fluid Mech., 53, pp. 257-284, 1994.
[12] Siddiqui A.M., Provost A., Schwarz W.H., Peristaltic pumping of a third- order fluid in a planar channel, Rheol. Acta, 32, pp. 47-56, 1993.
[13] Hayat T., Wang Y., Siddiqui A.M., Hutter K., Asghar S., Peristaltic transport of a third-order fluid in a circular cylindrical tube, Math. Models & Methods in Appl. Sci, 12, pp. 1691-1706, 2002.
[14] Haroun M.A., Effects of Deborah number and phase difference on peristaltic transport of a third order fluid in an asymmetric channel, Comm. Non linear sic. Nuber. Simul., 12, pp. 1464-1480, 2007.
[15] Subba Reddy M.V., Ramachandra Rao A., Sreenadh S., Peristaltic motion of a power law fluid in an asymmetric channel, Int. J. Non-Linear Mech., 42, pp.1153-1161, 2007.
[16] Nadeem S., Akram S., Peristaltic flow of a Williamson fluid in an asymmetric channel, Comm. Non linear sic. Numer. Simul., 15, pp.1705–1716, 2010.
[12] Mitra TK, Prasad SN, Journal of Biomechanics, 6, pp. 681-693, 1973.
[13] Mishra JC and Pandey SK , Mathematical and computer modelling,33,997-1009, 2001.
[14] Kavitha A, Hemadri Reddy R, Sreenadh S, Saravana R, Srinivas ANS, Advances in applied Science Research, 2(1), pp. 269-279, 2011.
[15] Hemadri Reddy R., Kavitha A., Sreenadh S., Hariprabhakaran P., Advances in applied Science Research, 2(2), pp. 167-178, 2011.
[16] Lakshminarayana P, Sreenadh S, Sucharitha G, Advances in Applied Science Research, 3(5), pp. 2890-2899, 2012.
[17] Radhakrishnamacharya G, Srinivasulu Ch, Computer Rendus Mecanique, 335, pp. 369-373, 2007.
[18] Rathod VP, Pallavi Kulkarni, Advances in applied Science Research, 2(3), pp. 265-279, 2011.
[19] Mokhtar A., Abd Elnaby, Haroun M.H., Communication in Nonlinear Science and Numerical simulation, 13, pp. 752-762, 2008.
[20] Srinivas S., Gayathri R., Kothandapani M., Computer Physics Communications, 180, pp. 2116-2112, 2009.
[26] Arun Kumar M., Sreenadh S., Srinivas S., Effects of wall properties and heat transfer on the peristaltic transport of a jeffrey fluid in a channel, *Advances in Applied Science Research*, 4(6), pp.159-172, 2013.
[27] Al-Khafajy D.G.S., Abdulhadi A.M., Effects of wall properties and heat transfer on the peristaltic transport of a jeffrey fluid through porous medium channel, Mathematical Theory and Modeling– IISTE, 4(9), pp. 86-99, 2014.